Aeroacoustics Conferences
26-29 May 2026, Brussels, Belgium
32nd AIAA/CEAS Aeroacoustics Conference (2026)

10.2514/6.2026-3333

Acoustic adjoint based methods for jet noise simulations

B. de Brye[1], N. Ghaisas[2], Y. Detandt[3]
Cadence Design Systems, Acoustic Division,1435 Mont-Saint-Guibert, Belgium

Stewart J. Leib[4]
HX5, LLC, NASA Glenn Research Center, Cleveland, Ohio, 44142, United States of America

É. Spieser[5] , C. Bailly[6]
École Centrale de Lyon, CNRS, Univ Claude Bernard Lyon 1, INSA Lyon, LMFA, UMR5509, 69130 Écully, France.

High fidelity jet noise simulations have been popular in the aeroacoustic community to better understand the various sound source mechanisms of open jets such as turbulence mixing noise, shock noise or entropy noise. Aircraft design trends lead to jets being installed closer to lifting devices causing important modifications in the radiated acoustic field. The present paper focuses on a technique to account for the propagation of sound for installed jets, assuming the noise sources are known. This work relies on the use of the reciprocity principle and the numerical computation of a tailored Green's function satisfying the adjoint problem. Starting from the linearized Euler's equations, the process is presented theoretically and then demonstrated on an isolated Mach 0.9 cold jet configuration. Acoustic monopoles are used to demonstrate the feasibility and the accuracy of the approach with known controlled sound sources.

I. Nomenclature

Ω = Acoustic volume
$\partial\Omega$ = Boundaries of the volume Ω
$\oint_{\partial\Omega} dx^2$ = Integral over the boundary surface defined by $\partial\Omega$
LEE = Linearized Euler Equations
Actran = Acoustic propagation simulation tool, solving scalar propagation wave in frequency domain
ActranDGM = Acosutic propagation simulation tool solving the LEE in the time domain.

II. Introduction

Since the 1950's, jet noise has been an important research topic for the aeroacoustics community, initially motivated to support the early development of jet aircraft engines. The understanding of source mechanisms and interactions leads to scaling laws and formulas driving, among other things, the aircraft evolution: modern engine designs are bigger in terms of diameter, with possible acoustic interactions with the lifting surfaces located close to

[1] Technical Leader, R&D Department, debrye@cadence.com.
[2] Acoustics Senior Engineer, R&D Department, nghaisas@cadence.com.
[3] Technical Director, R&D Department, ydetandt@cadence.com
[4] Senior Researcher, AIAA Senior Member .
[5] currently Research Engineer at: Département ERMES, EDF Lab Paris-Saclay, 91120 Palaiseau .
[6] Professor, Fluid Mechanics and Acoustics Laboratory (LMFA), AIAA Senior member.

the jet. Research is also strongly supported by numerical simulations, with an increasing fidelity in terms of turbulence modeling, therefore giving a better insight on source interaction mechanisms.

Simplified models are employed for jet noise predictions to provide sufficiently accurate results at lower cost and use fewer computational resources than high-fidelity simulations. For jet noise prediction, these reduced-order models are often based on an acoustic analogy. The original acoustic analogy of Lighthill [1] has provided significant insights into the physics of aerodynamically generated sound and has been used to make quantitative predictions of jet noise. It is an exact rearrangement of the governing equations, but several effects more properly associated with sound propagation are 'hidden' in its source terms.

Numerous researchers have since proposed alternative acoustic analogy formulations, many of which explicitly include the effects of sound propagation through a spatially varying flow. In these alternative analogies propagation effects are governed by a more complicated set of differential equations, generally some form of the linearized Euler equations (LEE), than the classical wave equation of Lighthill's analogy, necessitating either approximate or numerical solution. An example is the analogy formulation of Bogey, Bailly & Juvé [2].

Solutions of the propagation equations in acoustic analogy formulations are facilitated by use of a Green's function to obtain the fluctuating pressure as an integral of this fundamental solution multiplied by the source terms over the flow region. It was demonstrated by Tam & Auriault [3] that, in cases where the sources are distributed over a large volume but results are required only at a relatively small number of acoustic measurement points, there is a great computational advantage in solving the Green's function problem in its adjoint form [4].The adjoint method consists mainly in a mathematical generalization of the reciprocity principle, that enables the sound propagation to be computed from a receiver's perspective. Tam and Auriault [5] solved the adjoint of the linearized Euler's equations for a parallel base flow and applied their method to describe the effect of mean flow on the propagation of jet noise. More recent contributions have focused on numerically solving for the adjoint Green's functions and on the extension to other wave operators like Lilley's or Pierce's wave equations ([6], [7]). The latter approach has been implemented in the frequency domain with the solver Actran and demonstrated in [8] its ability to successfully account for complex installation effects such as the case of a round jet beneath a flat plate. Moreover, thanks to the technique, insight into some sound mechanisms of jets, such as upstream travelling guided jet waves, could be obtained [9].

However, noise predictions from previous studies ([5], [8], [9]) compare poorly with measurements around the peak noise direction near the jet axis. This is likely due to an oversimplified model for the sound source terms. More sophisticated models relying on realistic turbulence cross-correlations ([10], [11]) based on a generalised acoustic analogy [12], with sound propagation governed by a form of the linearized Euler's equations, may be more appropriate. In References [10] and [11] noise predictions were obtained for an isolated jet using this generalised acoustic analogy with propagation effects computed numerically for a locally parallel axisymmetric mean flow. Accurate predictions for more complex geometries, including installation effects, require a more general and robust numerical approach for modelling sound propagation.

In this paper we present a general formulation for the adjoint Green's function problem of the LEE and demonstrate a numerical technique for its solution on a baseline axisymmetric jet test case. The numerical technique is based on the Discontinuous Galerkin Method and implemented into the acoustic simulation software ActranDGM [13] . This work is a first step in implementing a RANS-based noise prediction module for sheared mean flows within ActranDGM.

The acoustic measurement points are generally located far from the jet, outside of the region where fluid simulations can capture the acoustics accurately and efficiently. The acoustic solutions are generally computed from the fluid results with integral solutions, where the source information is weighted by transfer functions and integrated over a volume and/or surface depending on the formulation. This is discussed in Section III. This transfer function is Green's solution to the adjoint problem described in Section IV. The solution for the acoustic pressure in the case where source terms are present only in the momentum equation is given in Section V. The test case used to demonstrate the method is described in Section VI and results are presented in Section VII. Concluding remarks are made and plans for future work are discussed in Section VIII.

III. Integral solution for jet noise

The present section recalls the concepts of a Green's function to solve acoustic problems. Let's denote by q_i the acoustic unknowns (namely the density, velocity components and pressure fluctuations), satisfying a set of equations defined by vectorial operator $\mathcal{L}_i$

$$\mathcal{L}_i(\vec{q}) = -I\omega q_i + \frac{\partial}{\partial x_j}\left(F_{ik}^j q_k\right) + R_{ik} q_k = S_i \tag{1}$$

with $I^2 = -1$ and $\omega = 2\pi f$ is the radian frequency. For jet noise, the Linearized Euler Equations (LEE) are commonly adopted to propagate acoustics in complex mean flows. The solution depends on the spatial position $\vec{x}$ and frequency f. The boundary conditions are

$$\bar{Z}_{ij} q_j = \bar{q}_i \text{ on } \partial\Omega \quad , \tag{2}$$

on any surfaces $\partial\Omega$ and an outgoing wave condition for $|\vec{x}| \to \infty$.

This problem is presented in the frequency domain, but the development remains similar in the time domain. To solve this problem by an integral solution, we seek a solution $q_i^{\blacksquare}(\vec{x},\vec{y},\omega)$ satisfying the adjoint problem defined by

$$\mathcal{L}_i^{\blacksquare}\left(\overrightarrow{q_\alpha^{\blacksquare}}\right) = I\omega q_{i\alpha}^{\blacksquare} + \frac{\partial}{\partial x_j}\left(\mathcal{F}_{ik}^j q_{k\alpha}^{\blacksquare}\right) + \mathcal{R}_{ik} q_{k\alpha}^{\blacksquare} = \delta_{i\alpha}(\vec{x}-\vec{y}) \quad , \tag{3}$$

where $\delta_{i\alpha}(\vec{x}-\vec{y})$ is a Dirac function acting at point $\vec{x}=\vec{y}$ if $i=\alpha$ and 0 everywhere if $i \neq \alpha$. The $\mathcal{L}_i^{\blacksquare}\left(\overrightarrow{q_\alpha^{\blacksquare}}\right)$ is the adjoint operator yielding the integral solution formula:

$$q_\alpha(\vec{y},\omega) = \int \left(\left(q_{i\alpha}^{\blacksquare}(\vec{x},\vec{y},\omega)\right)^* \cdot S_i(\vec{x},\omega)\ dx^3 \quad , \tag{4}$$

where $*$ denotes the complex conjugate, provided we can find the solution $q_{i\alpha}^{\blacksquare}$ at point $\vec{x}$ due to a source located at point $\vec{y}$ for a Dirac impulse $\delta\ \ (\vec{x}-\vec{y})$ in equation $i = \alpha$. The adjoint problem is similar to the original problem (1), except that the operator $\mathcal{L}_i^{\blacksquare}$ may be different from $\mathcal{L}_i$ and the source term is an impulse at position $\vec{y}$ in the α^{th} equation. The solution is called adjoint Green's function in the remaining part of the document.

Mathematically speaking, the adjoint problem is defined by an operator $\mathcal{L}_i^{\blacksquare}$, similar to the one of the original problem $\mathcal{L}_i$, and satisfying Green-Lagrange's identity:

$$\int q_i\left(\mathcal{L}_i^{\blacksquare}(\vec{q}_\alpha^{\blacksquare})\right)^* dx^3 = \int (q_{i\alpha}^{\blacksquare})^* \mathcal{L}_i(\vec{q})\ dx^3 \quad . \tag{5}$$

Because the solution of the problem is sought in the frequency domain, a Hermitian scalar product is used. Hence, the term $+I\omega$ used in equation (3). This identity defines the mathematical relation between the matrices $\mathcal{F}_{ik}^j$ and F_{ik}^j and $\mathcal{R}_{ik}$ and R_{ik}, and also sets the boundary conditions for $q_{i\alpha}^{\blacksquare}$ on $\partial\Omega$:

$$\mathcal{F}_{ik}^j = -F_{ki}^j \quad , \tag{6}$$

$$\mathcal{R}_{ik} = R_{ki} + \frac{\partial F_{ki}^j}{\partial x_j} \quad , \tag{7}$$

and

$$\mathcal{F}_{ik}^j q_{k\alpha}^{\blacksquare} n_j = 0 \quad . \tag{8}$$

Solving the adjoint problem (i.e. satisfying Eq. (3) and (8)) is typically as complex as solving the original problem (Eq. (1) and (2)). If one finds a solution of Eq. (3), not satisfying the boundary condition Eq. (8), the integral solution Eq. (4) becomes :

$$q_\alpha(\vec{y},\omega) = \int \left(\left(q_{i\alpha}^{\blacksquare}(\vec{x},\vec{y},\omega)\right)^* \cdot S_i(\vec{x},\omega)\ dx^3 + \oint_{\partial\Omega} \mathcal{F}_{ik}^j q_i q_{k\alpha}^{\blacksquare} \widehat{n_j} dx^2 \tag{9}$$

where $\oint_{\partial\Omega} dx^2$ is the integral over any surfaces in the volume analyzed and $\widehat{n_j}$ are the unit normal vectors to these surfaces. In very few configurations, the governing equations for acoustic wave propagation (Eq. (1)) leads to an analytical expression for $q_{i\alpha}^{\blacksquare}(\vec{x},\vec{y},\omega)$ satisfying Eq. (3). The boundary conditions are generally not satisfied, leading to an implicit formulation as indicated by Eq. (9).

IV. Linearized Euler equations

The non-conservative form of the linearized Euler equations are recalled here in the frequency domain. This set of equations considers the five acoustic fluctuations unknowns (density ρ, velocity components v_i and pressure p). The five equations are arranged in the vectorial operator $\mathcal{L}_i$ as:

- Continuity equation in row *i=0*,
- Momentum equations in *i=1,2,3*
- Energy equation in row *i=4*

$$\vec{q} = \begin{pmatrix} \rho \\ v_1 \\ v_2 \\ v_3 \\ p \end{pmatrix} \quad (10a) \qquad \mathcal{L}_i(\vec{q}) = \begin{pmatrix} -I\omega\rho + \dfrac{\partial}{\partial x_j}\left(\rho v_j^0 + \rho^0 v_j\right) = S_0 \\ -I\omega v_1 \ + v_j^0 \dfrac{\partial v_1}{\partial x_j} + v_j \dfrac{\partial v_1^0}{\partial x_j} + \dfrac{1}{\rho^0}\dfrac{\partial p}{\partial x_1} + \dfrac{\rho}{(\rho^0)^2}\dfrac{\partial p^0}{\partial x_1} = S_1 \\ -I\omega v_2 \ + v_j^0 \dfrac{\partial v_2}{\partial x_j} + v_j \dfrac{\partial v_2^0}{\partial x_j} + \dfrac{1}{\rho^0}\dfrac{\partial p}{\partial x_2} + \dfrac{\rho}{(\rho^0)^2}\dfrac{\partial p^0}{\partial x_2} = S_2 \\ -I\omega v_3 \ + v_j^0 \dfrac{\partial v_3}{\partial x_j} + v_j \dfrac{\partial v_3^0}{\partial x_j} + \dfrac{1}{\rho^0}\dfrac{\partial p}{\partial x_3} + \dfrac{\rho}{(\rho^0)^2}\dfrac{\partial p^0}{\partial x_3} = S_3 \\ -I\omega p + \dfrac{\partial}{\partial x_j}\left(p v_j^0 + \rho^0 c^2 v_j\right) + (1-\gamma)\dfrac{\partial p^0}{\partial x_j} v_j - p\dfrac{\partial v_j^0}{\partial x_j} = S_4 \end{pmatrix} \quad (10b)$$

where the superscript "0" denotes the time-averaged steady field supporting the acoustic propagation and $\gamma$is the ratio of specific heats. For the form of the LEE in equations (10), the coefficient matrices F_{ik}^j and R_{ik} are:

$$F_{ik}^j = \begin{pmatrix} v_j^0 & \rho^0\delta_{1j} & \rho^0\delta_{2j} & \rho^0\delta_{3j} & 0 \\ 0 & v_j^0 & 0 & 0 & \dfrac{\delta_{1j}}{\rho^0} \\ 0 & 0 & v_j^0 & 0 & \dfrac{\delta_{2j}}{\rho^0} \\ 0 & 0 & 0 & v_j^0 & \dfrac{\delta_{2j}}{\rho^0} \\ 0 & \rho^0 c^2\delta_{1j} & \rho^0 c^2\delta_{2j} & \rho^0 c^2\delta_{3j} & v_j^0 \end{pmatrix} \quad \text{with} \quad \delta_{ij} = \begin{matrix} 1 & \text{if } i = j \\ 0 & \text{if } i \neq j \end{matrix} \qquad , \qquad (11)$$

and

$$R_{ik} = -\begin{pmatrix} 0 & 0 & 0 & 0 & 0 \\ \frac{p_1^0}{(\rho^0)^2} & \Delta - \frac{\partial v_1^0}{\partial x_1} & -\frac{\partial v_1^0}{\partial x_2} & -\frac{\partial v_1^0}{\partial x_3} & \rho_1^0 \\ \frac{p_2^0}{(\rho^0)^2} & -\frac{\partial v_2^0}{\partial x_1} & \Delta - \frac{\partial v_2^0}{\partial x_2} & -\frac{\partial v_2^0}{\partial x_3} & \rho_2^0 \\ \frac{p_3^0}{(\rho^0)^2} & -\frac{\partial v_3^0}{\partial x_1} & -\frac{\partial v_3^0}{\partial x_2} & \Delta - \frac{\partial v_3^0}{\partial x_3} & \rho_3^0 \\ 0 & \rho^0\frac{\partial c^2}{\partial x_1} & \rho^0\frac{\partial c^2}{\partial x_2} & \rho^0\frac{\partial c^2}{\partial x_3} & \Delta + \frac{c^2}{p^0} v_j^0 \frac{\partial \rho^0}{\partial x_j} \end{pmatrix} \quad \text{with} \quad \begin{matrix} p_i^0 = \frac{\partial p^0}{\partial x_i} \\ \rho_i^0 = -\frac{1}{(\rho^0)^2}\frac{\partial \rho^0}{\partial x_i} \\ \Delta = \frac{\partial v_i^0}{\partial x_i} \end{matrix} \quad , \qquad (12)$$

where $c^2 = \left(\frac{\partial p}{\partial \rho}\right)_s$ is the square of the mean speed of sound.

The adjoint problem is defined by the matrices $\mathcal{F}_{ik}^j$ and $\mathcal{R}_{ik}$ and the formulas in equations (6) to (8). The present paper solves the adjoint problem numerically by modifying the set of equations solved by ActranDGM and finding the so-called adjoint tailored Green's function which satisfies Eq. (3) and the boundary conditions Eq. (8), leading to an explicit integral solution Eq. (4).

Actran DGM [13] is an adaptive high-order Discontinuous Galerkin finite element solver for the Linearized Euler Equations (LEE) in the time domain for homentropic or isentropic flows. Gaussian quadrature or quadrature-free integration methods are possible; in this study we focus on the quadrature-free form for faster iteration time reasons.

Tetrahedral elements are used for three-dimensional configurations while triangular elements handle two-dimensional or axisymmetric computations. Time integration is performed with an explicit low-dissipation, low-dispersion Runge-Kutta scheme. Polynomial orders ranging from 1 to 16 are assigned locally and automatically based on the target frequency (f), the local element size, the local speed of sound (c) and the local mean flow convection (u_0), using the most restrictive upstream-propagating acoustic wavelength $\lambda = (c - u_0)/f$ as the resolution criterion. The numerical flux at element interfaces is handled with various Riemann solvers (exact upwind, Harten, Lax and van Leer [HLL], Lax Friedriechs,…). In this study the HLL flux is used. Boundary conditions include rigid walls, absorbing buffer zones, impedance/admittance conditions with Myers term support, and acoustic duct mode injection. While the DG discretisation increases the total number of degrees of freedom compared to a continuous Galerkin approach, it offers several algorithmic advantages. The element-wise discontinuities confine MPI inter-process communication to face-neighbour exchanges, yielding efficient domain-decomposition parallelism. Operating at high polynomial order on small, dense element matrices leverages GPU acceleration effectively. Finally, with an explicit time scheme the global mass matrix is block-diagonal and can be inverted element-by-element, reducing the system solution step to a sequence of dense matrix-matrix multiplications (GEMM), which execute at near-peak hardware throughput on both CPU (with Blas library) and GPU architectures (with cuBlas library).

The source terms, denoted by S_i in equations (10b), correspond to the excitation of the system. For turbulent flows, these terms provide the unsteady volume excitation from the unsteady flow field. In classical hybrid aeroacoustic theory, these terms are defined as the non-linear Navier-Stokes (or Euler) residuals for an acoustic propagation operator defined on the left hand side of equations. This was discussed and presented in detail in [2] and [14]. Following [2] and [14], source terms are retained only in the momentum equation and these can be written as:

$$\vec{S} = \begin{pmatrix} 0 \\ \dfrac{1}{\rho^0}\left(\dfrac{\partial(\rho v_i v_1)^0}{\partial x_i} - \dfrac{\partial \rho v_i v_1}{\partial x_i}\right) \\ \dfrac{1}{\rho^0}\left(\dfrac{\partial(\rho v_i v_2)^0}{\partial x_i} - \dfrac{\partial \rho v_i v_2}{\partial x_i}\right) \\ \dfrac{1}{\rho^0}\left(\dfrac{\partial(\rho v_i v_3)^0}{\partial x_i} - \dfrac{\partial \rho v_i v_3}{\partial x_i}\right) \\ 0 \end{pmatrix} = \begin{pmatrix} 0 \\ \dfrac{1}{\rho^0}\dfrac{\partial e'_{i1}}{\partial x_i} \\ \dfrac{1}{\rho^0}\dfrac{\partial e'_{i2}}{\partial x_i} \\ \dfrac{1}{\rho^0}\dfrac{\partial e'_{i3}}{\partial x_i} \\ 0 \end{pmatrix} \quad \text{with} \qquad e'_{ij} = (\rho v_i v_1)^0 - \rho v_i v_1 \quad . \tag{13}$$

Other sources may apply and play a role in the energy equation and momentum equations (combustion) but will not be discussed here.

V. Source Modeling

According to eq. (13), the turbulent noise sources contribute only in the momentum equation, not in the continuity or energy equations (*ie.* $S_0 = S_4 = 0$). The computation of the acoustic pressure in this case simplifies to the following expression

$$p(\vec{y}, \omega) = \int \left(\left(q^{\blacksquare}_{i4}(\vec{x}, \vec{y}, \omega) \right)^* \cdot S_i(\vec{x}, \omega) \; dx^3 = \int \left((v^{\blacksquare}_{14})^* S_1 + (v^{\blacksquare}_{24})^* S_2 + (v^{\blacksquare}_{34})^* S_3 \right) \; dx^3 \tag{14}$$

where $q^{\blacksquare}_{i4}(\vec{x}, \vec{y}, \omega) = (\rho^{\blacksquare}_4, \quad v^{\blacksquare}_{14}, \quad v^{\blacksquare}_{24}, \quad v^{\blacksquare}_{34}, \quad p^{\blacksquare}_4)^{\mathrm{t}}$ is the solution of the adjoint problem defined by

$$I\omega q^{\blacksquare}_{i4} + \frac{\partial}{\partial x_j}\left(\mathcal{F}^j_{ik} q^{\blacksquare}_{k4}\right) + \mathcal{R}_{ik} q^{\blacksquare}_{k4} = \delta_{i4}(\vec{x} - \vec{y}). \tag{15}$$

From the solution for the acoustic pressure, a formula for the acoustic spectral density can be written in terms of the adjoint Green's function and the cross-correlation of the source terms

$$I_\omega(\vec{y}) = \int_V \int_V \frac{\partial \hat{q}^{\blacksquare}_{i4}}{\partial x_j}(\vec{x} | \vec{y}, \omega) \frac{\partial \hat{q}^{\blacksquare}_{k4}}{\partial \xi_l}^{*} \left(\vec{x} + \vec{\xi} | \vec{y}, \omega\right) H^*_{ijkl}\left(\vec{x}, \vec{\xi}, \omega\right) dx^3 d\xi^3 \,, \tag{16}$$

where

$$H_{ijkl}(\vec{x},\vec{\xi},\omega) = \int_{-\infty}^{\infty} e^{i\omega\tau} R_{ijkl}(\vec{x},\vec{\xi},\tau) d\tau \,, \tag{17}$$

with

$$R_{ijkl}(\vec{x},\vec{\xi},\tau) = \frac{1}{2T}\int_{-T}^{T} e'_{ij}(\vec{x}, t) e'_{kl}(\vec{x}+\vec{\xi}, t+\tau) dt \,, \tag{18}$$

if mean density gradients are neglected in the source terms.

Equations (16) – (18) provide a formula for computing the acoustic spectrum in terms of the solution to the adjoint Green's function component, $q_{k4}^{\blacksquare}$, and the cross-correlations of the source terms in the second element of (13). Models for these cross correlations have been developed in [5] and [11], for example.

VI. Illustration Testcase

The test case used in this paper corresponds to a jet issuing from the baseline round Small Metal Chevron (SMC000) nozzle, used extensively at NASA Glenn Research Center ([15], [16]), at Nozzle Pressure Ratio (NPR) of 1.854 and Nozzle Temperature Ratio (NTR) of 1.0. This is a convergent nozzle with exit diameter, D , of two inches and is pictured in Figure 1. The flow and noise characteristics of this nozzle have been well documented experimentally under a wide range of flow conditions. The case here, which corresponds to a near-sonic, cold exit condition, $M_a = U_J / c_\infty = 0.9$, $T_J / T_\infty = 0.81$, where M_a is the acoustic Mach number, U_J is the jet exit velocity, c_∞ the ambient speed of sound, T_J the jet exit temperature, and T_∞ the ambient temperature, is referred to as Set Point 7.

Figure 1: Baseline Small Metal Chevron (SMC000) Nozzle.

A Reynolds-averaged Navier-Stokes (RANS) solution is available for this jet case computed using the Wind-US code ([17],[18]). The solution has been compared with experimental data taken at NASA Glenn and found to provide reasonably good agreement with the measured mean flow velocity and turbulent kinetic energy, k . It has been used in the jet noise predictions presented in reference [10] and [11]. Figure 2 shows contours of mean streamwise velocity, normalized by the ambient sound speed, and turbulent kinetic energy, normalized by the jet exit velocity, in the axial-radial plane from this solution. The mean velocity and mean temperature from this RANS solution are used in adjoint Green's function calculations presented in this paper.

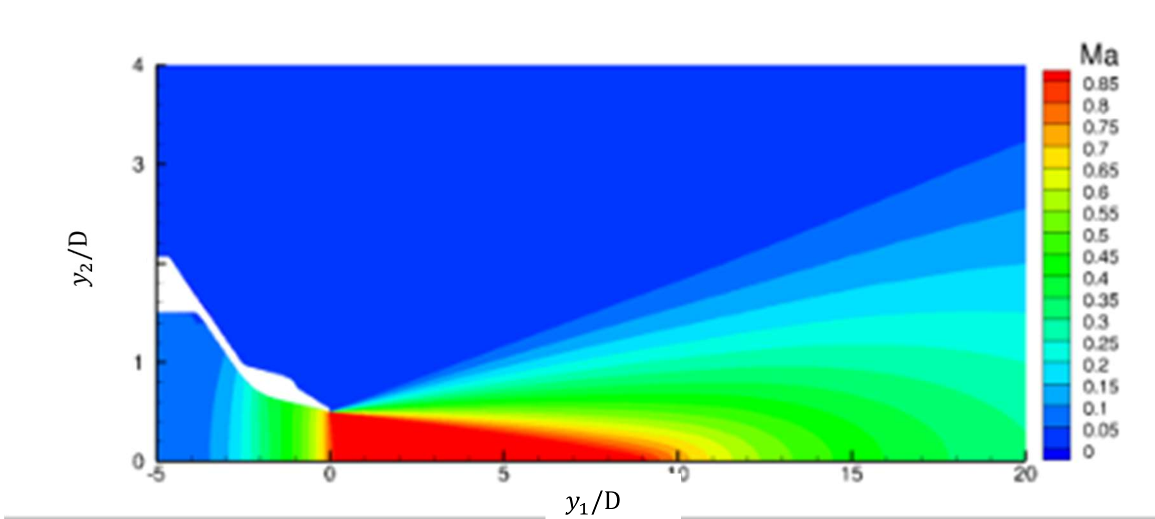

(a)

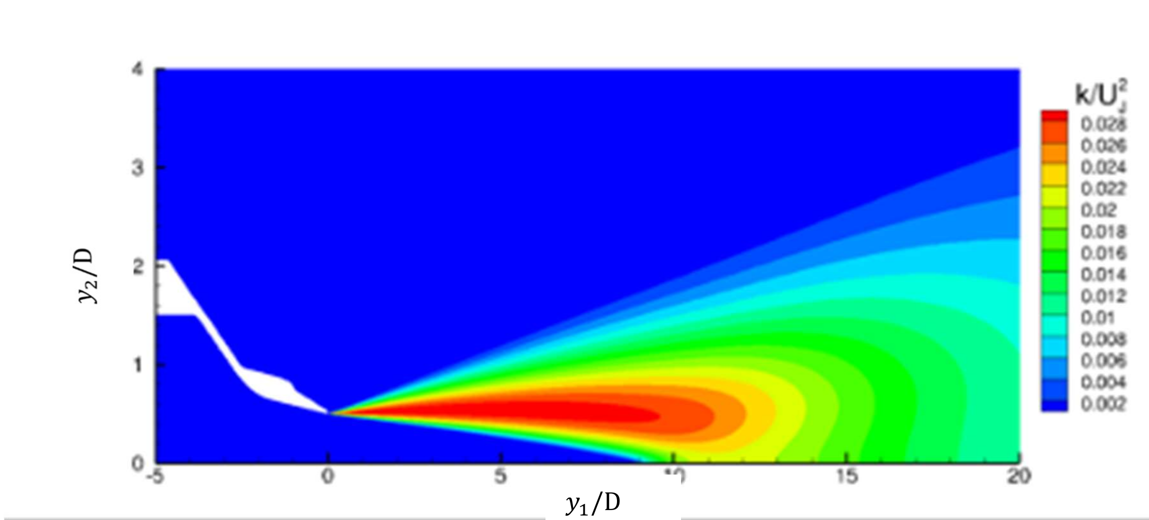

(b)

Figure 2: (a) Normalized Mean Streamwise Velocity (Acoustic Mach Number), (b) Normalized Turbulent Kinetic Energy from a Wind-US RANS solution.

VII.Results

The computations target acoustic frequencies between 1 kHz and 8 kHz, in increments of 1 kHz, corresponding to Strouhal numbers $St = fD/U_J$ ranging from 0.16 to 1.28. Three 3D meshes were generated to accommodate this frequency range:

- a coarse mesh for 1–3 kHz,
- an intermediate mesh for 4–6 kHz (Figure 3),
- a fine mesh for 7–8 kHz.

The same mesh is used for adjoint computation and for direct computations at the target frequency. For all meshes, the characteristic element size Δ is prescribed as $\Delta = 0.2\lambda_{\min}$, and the absorbing buffer thickness δ as $\delta = 3\lambda_{\max}$, where $\lambda_{\min}$ and $\lambda_{\max}$ correspond to the minimum and maximum wavelengths of the target frequency band, respectively.

Near the nozzle exit, the mesh resolution is further constrained by the local geometry, with $\Delta = 0.5 r_{\min}$, where $r_{\min}$ denotes the minimum duct radius.

Five microphone positions are arranged along an arc in the upper $y_1 - y_2$ plane, and three acoustic sources are located in the same plane around the jet plume (refer to Figure 3) and the simulations consider the full 3D geometry and flow (3D simulations). The adjoint solutions are computed with a source in the continuity equation ($\alpha = 0$ in equation (3)).

To mitigate instability waves arising from steep mean flow gradients in the jet shear region (Kevin-Helmholtz oscillations, denoted KH), a homentropic formulation is adopted. In the core jet region of the domain (colored red in Figure 3), the mean flow gradients are artificially suppressed, and a vortical diffusive limiter, analogous to the artificial damping term (ADT) approach described in [18], is activated to enhance robustness. Furthermore, the total physical time is kept as small as possible to avoid too high amplitude for KH oscillations.

Figure 3 presents a $y_1 - y_2$ slice of the intermediate mesh used for the 4–6 kHz computations. The buffer region is shown in green, the physical domain in blue, and the limiter-activated region in red. Source locations (monopole or dipole) are indicated by yellow markers (S1, S2, S3), and microphone positions by blue markers (M1–M5). Micro and source coordinates are given in Table 1.

Table 1: Micro and source positions in meters, the row R/D= $\frac{\sqrt{y_1^2+y_2^2+y_3^2}}{D}$ gives the distance from nozzle in nozzle diameter and the row θ gives the polar angle in degrees

	M1	M2	M3	M4	M5	S1	S2	S3
y_1	1.940	1.632	1.129	0.580	0.0	0.92	0.92	0.92
y_2	0.195	0.698	0.950	1.133	1.213	0.56	0.0	-0.56
y_3	0.0	0.0	0.0	0.0	0.0	0.0	0.0	0.0
R/D	36.79	33.49	27.84	24.02	22.89	20.32	17.36	20.32
θ	5.74	23.16	40.08	62.89	90.00	31.33	0.00	-31.33

For direct Green's function solutions, one computation is required per source. In contrast, for the adjoint Green's function, one computation is performed per microphone position and the solution is obtained at all source locations within the computational mesh. The maximum physical simulation time is set to 0.015 s. Table 2 summarizes, for each frequency, the number of mesh elements, the associated degrees of freedom, and the CPU time per source (direct run) or per microphone (adjoint run).

For this study, we focus on the acoustic pressure at the microphones, so only one computation with the adjoint formulation is needed for each observer. Each of these computations is excited with a mass monopole (in the homentropic flow formulation) at the microphone position, which is referred to as the radiation sequence in Actran DGM. The natural frequencies of the time domain solution are computed with a least square technique to accuractely select the frequencies on a signal not spanning over an exact multiple of periods. The acoustic pressure frequency response at the microphones (M1–M5) is then evaluated using this adjoint Green's function solution in the integral of equation (14) with mass monopoles (Dirac delta functions)for the sources S1, S2, S3 (in the solution sequence in Actran DGM). This acoustic pressure response computed using the adjoint Green's function is then compared to that obtained using with classical direct Green's function approach.

Computations are launched sequentially using NVIDIA Grace Hopper GH200 nodes taking advantage of the GPU acceleration. Speedup gains are substantial, i.e the iteration times are reduced by a factor ~100 compared to a single process computation in the same node.

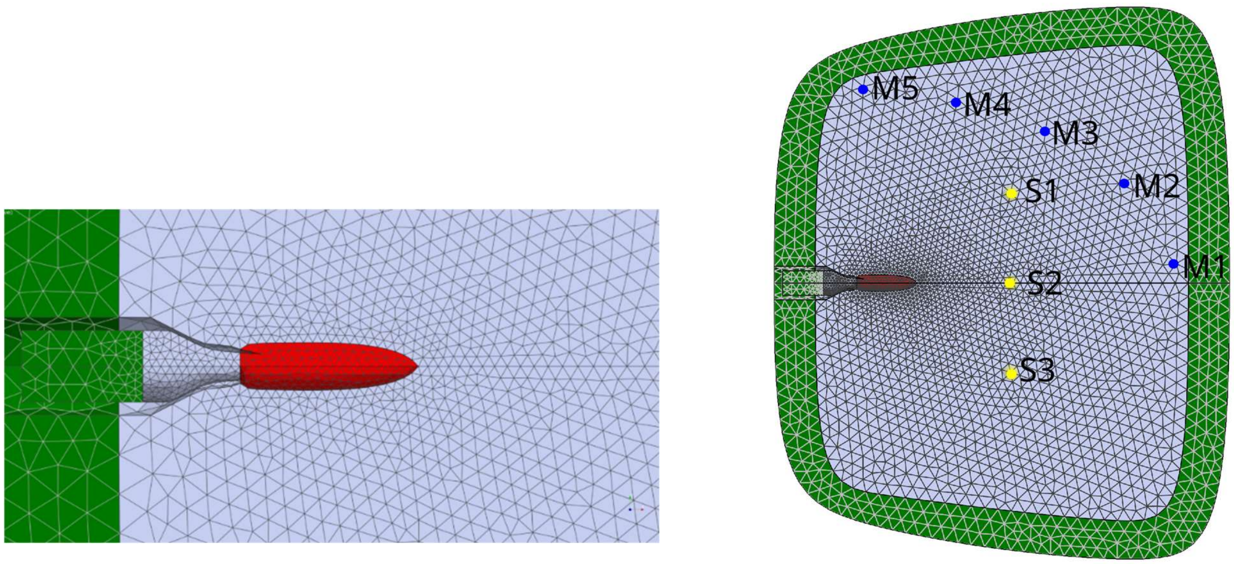

Figure 3: $y_1 - y_2$ cut view of the intermediate mesh (f=[3; 4; 5]kHz). The mesh colored in green is a sponge zone damping the outgoing waves, the mesh colored in blue is the region where the Linearized Euler/Adjoint equations are solved, the red colored part is where a limiter (diffusion term based on local instabilities [18]) is active to reduce the Kelvin-Helmholtz instabilities amplitudes.

Table 2: Computational characteristics for the different simulations

		Number		
Source frequency	Strouhal number *St*	Elements	Degrees of Freedom	CPU time on GH200
1kHz	0.16	89,072	13,687,936	8m
2kHz	0.32	89,072	29,060,772	22m
3kHz	0.48	89,072	50,882,456	33m
4kHz	0.64	229,396	89,994,680	3h 21m
5kHz	0.80	229,396	120,360,972	3h 52m
6kHz	0.96	229,396	159,469,956	6h 50m
7kHz	1.12	623,668	317,349,844	7h 10m
8kHz	1.28	623,668	402,939,284	8h 20m

The main objective of these simulations is to demonstrate the equivalence of acoustic pressure response using the direct and the adjoint Green's function approachs:

- The direct approach is solved with monopole sources set at points S1 (blue), S2 (red) and S3(green) and the acoustic pressure is computed at M1-M5
- The adjoint approach is computed using the solution $q_{i0}^{\blacksquare}(\vec{x},\vec{y},\omega)$ of adjoint problem (3), for a monopole source located in the continuity equation and computing the pressure from $p = c^2\rho$

The simulations are performed in the time domain for sources acting at a single frequency to isolate the process. Both direct and adjoint simulations could be performed for multiple frequencies at a time, on the same mesh, speeding up the simulations.

Figure 4 shows directivities of the acoustic pressure obtained using the direct and adjoint solutions and suggest good agreeement, except for the frequencies 2000Hz and 3000Hz for which the development of Kelvin-Helmholtz instability waves generates differences. These results illustrate the validity of the approach; the acoustic directivity is recovered using the adjoint method and the source definition, even in the presence of a strongly sheared mean flow.

We note that the adjoint Green's solution could be pre-computed and stored for use in subsequent simulations using different source specifications.

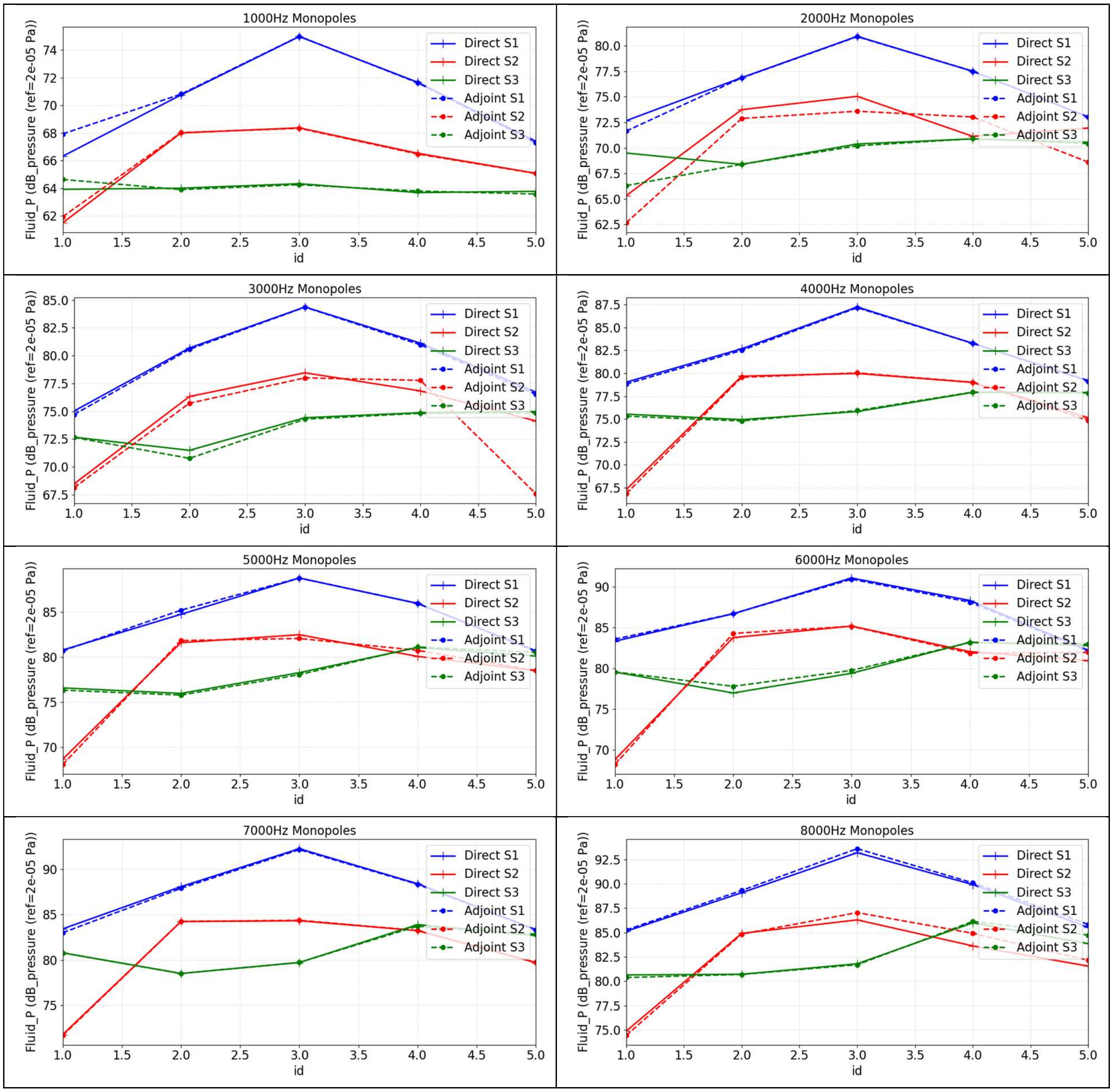

Figure 4: Monopole results for direct and adjoint computation for the 3 monopoles S1, S2 and S3 at the 5 micro positions (from 1kHz to 8kHz).

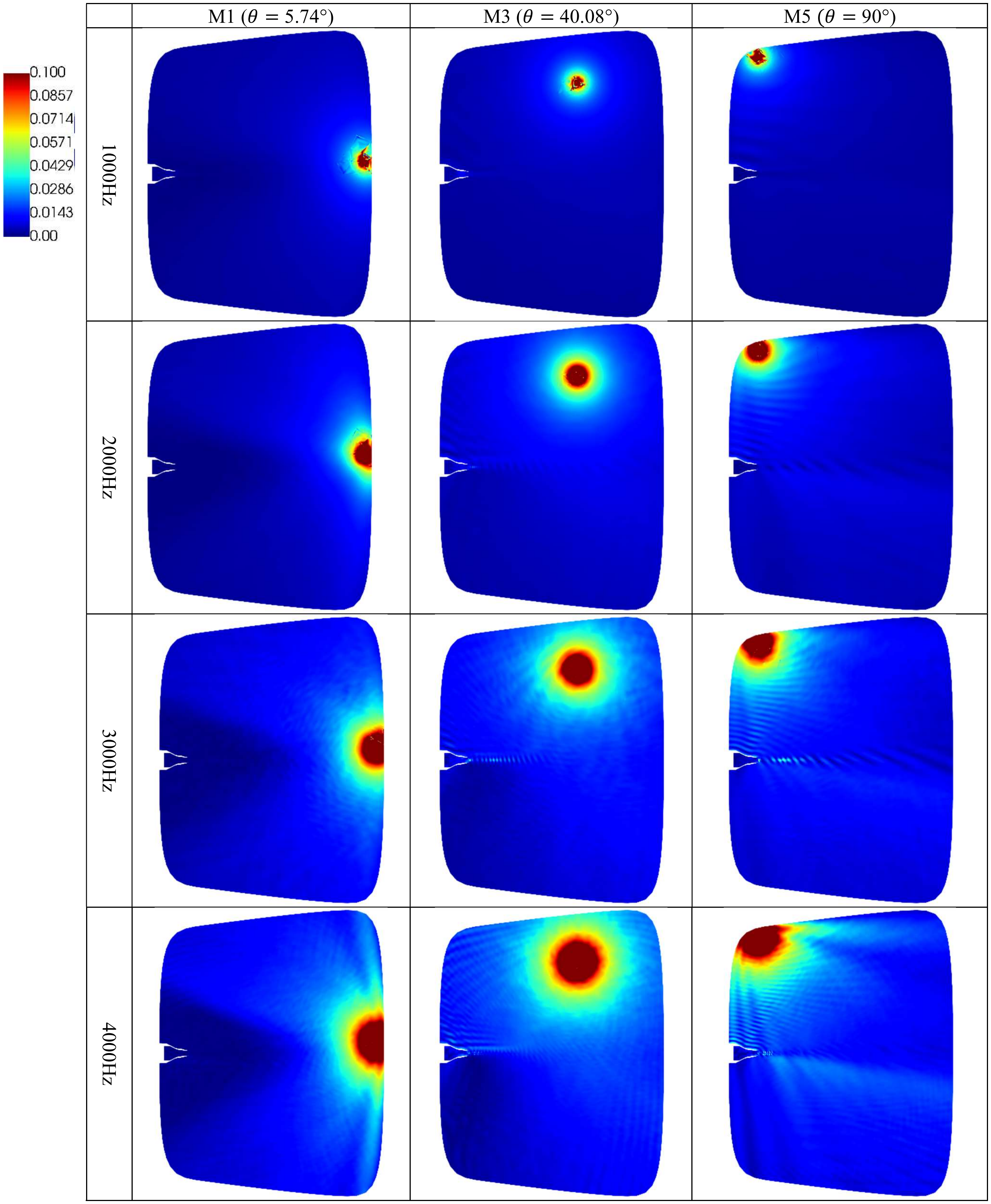
M1 ($\theta = 5.74°$)
M3 ($\theta = 40.08°$)
M5 ($\theta = 90°$)
1000Hz
2000Hz
3000Hz
4000Hz
0.100
0.0857
0.0714
0.0571
0.0429
0.0286
0.0143
0.00

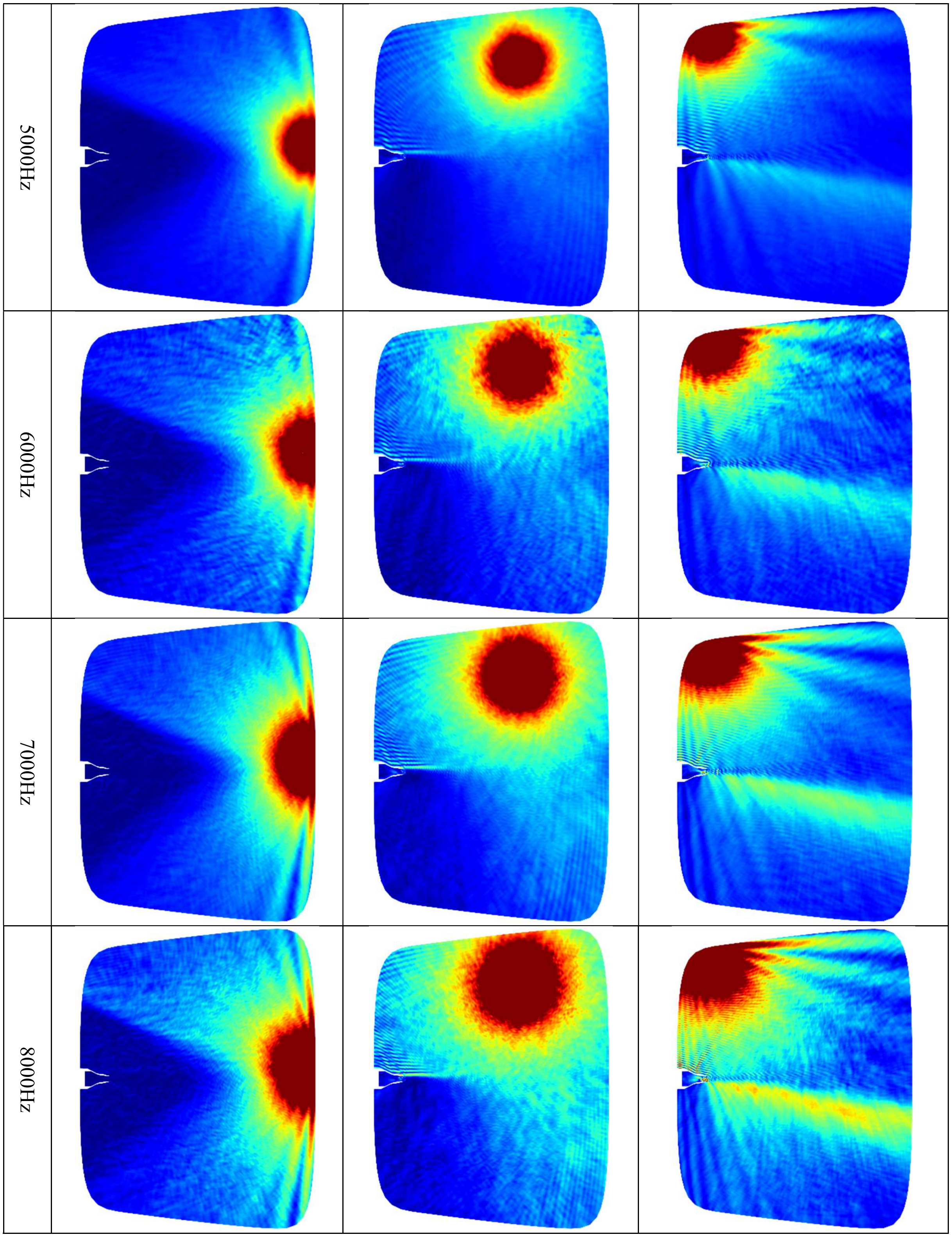

Figure 5: Amplitude of adjoint Green's solution $c^2 q^{\blacksquare}_{00}(\vec{x}, \vec{y} = M_i, \omega)$ for a Dirac impulse located at $\vec{y} = M_1$ (left column), $\vec{y} = M_3$ (middle column) and $\vec{y} = M_5$M5 (right column) between 1kHz to 8kHz. The solution is cropped between 0 and 0.1

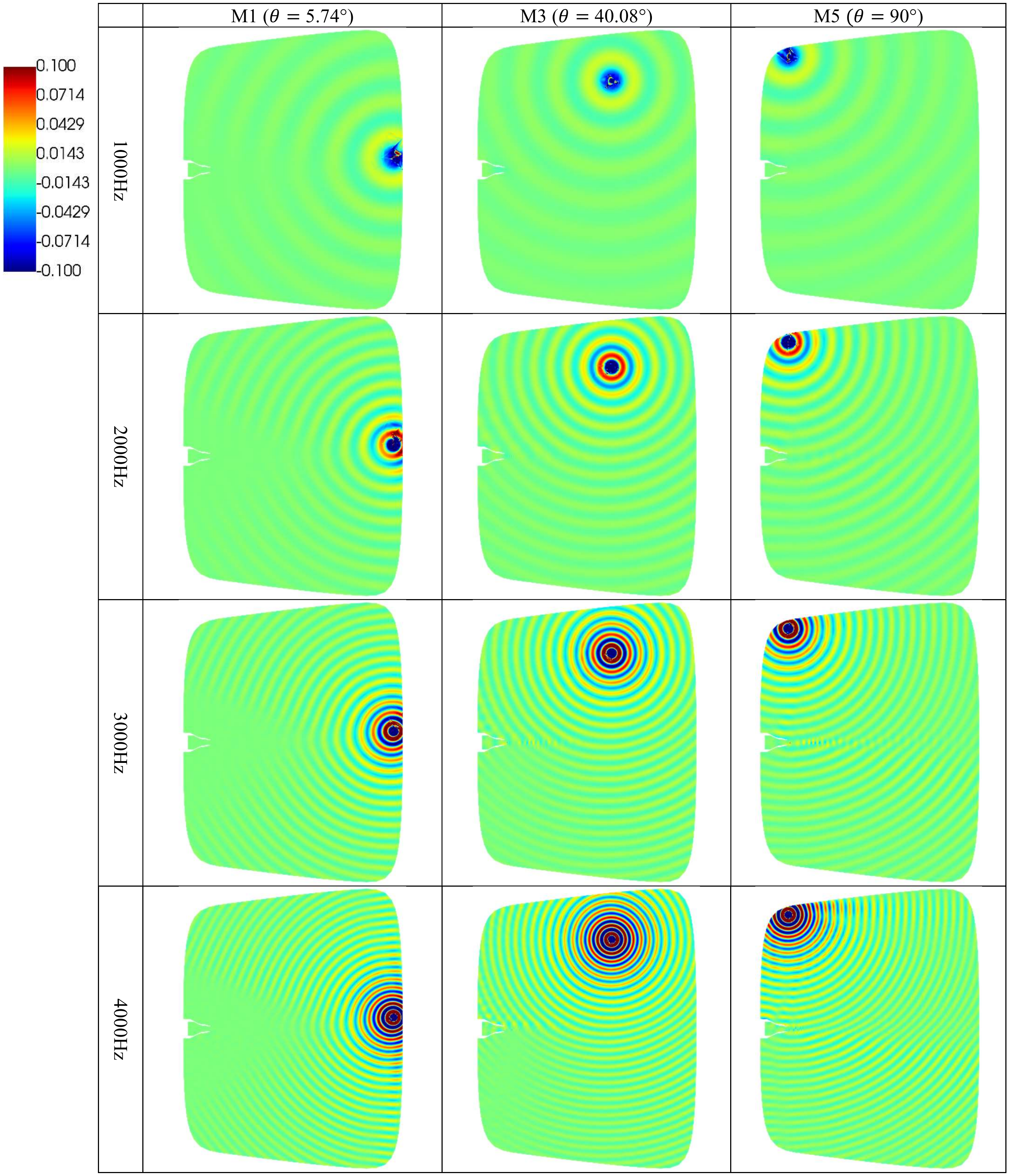
M1 ($\theta = 5.74°$)
M3 ($\theta = 40.08°$)
M5 ($\theta = 90°$)
1000Hz
2000Hz
3000Hz
4000Hz
0.100
0.0714
0.0429
0.0143
-0.0143
-0.0429
-0.0714
-0.100

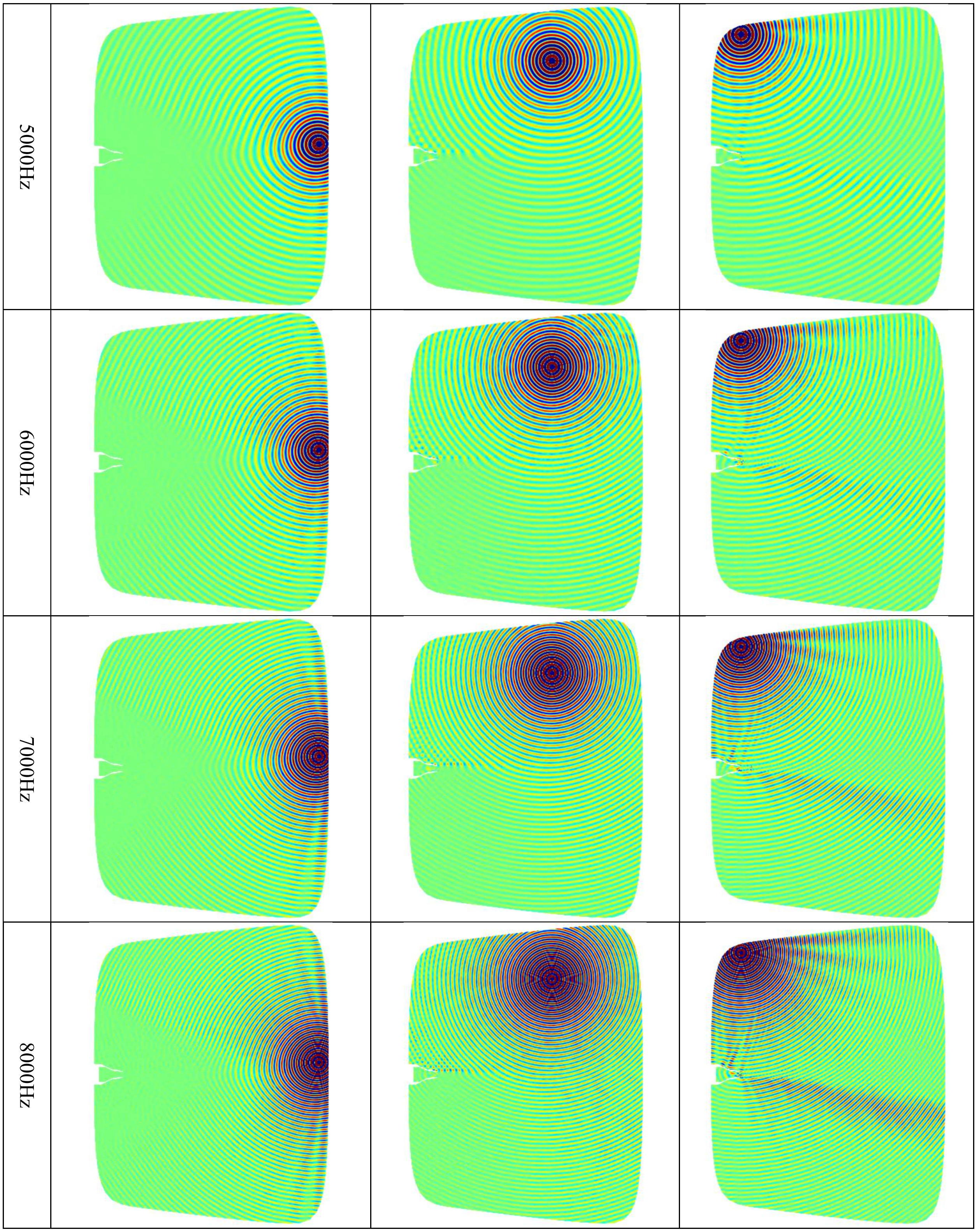

Figure 6 Real part of adjoint Green's solution $c^2 q^{\blacksquare}_{00}(\vec{x},\vec{y},\omega)$ for a Dirac impulse located at $\vec{y} = M_1$ (left column), $\vec{y} = M_3$ (middle column) and $\vec{y} = M_5$ (right column) between 1kHz to 8kHz. The solution is cropped between -0.1 and 0.1

Figure 5 and Figure 6 present maps of the adjoint Green's function $c^2 q_{00}^{\blacksquare}$ for sources located at the M1, M3 and M5 microphones, respectively. This adjoint solution weights the source contributions in equation (14) and could be seen as the sensitivity map at position $\vec{y}$ for sources at points $\vec{x}$ located anywhere in the jet flow. If the map level at a point $\vec{x}$ is large, this means any source located at this position $\vec{x}$ will have a significant contribution to the noise heard at $\vec{y}$.

For the results corresponding to the threemicrophone positions shown in Figure 5 and 6, little effect of the jet flow or duct wall can be seen on the adjoint solution computed at low frequencies ($f \leq 3000Hz$) and the solution seems to behave like a simple acoustic monopole. For higher frequencies ($f \geq 5000Hz$) the pattern shows some preferred directions and a specific region aligned with the jet flow shear layer is visible. This zone, for which the amplitude of adjoint Green's function is higher, corresponds to a region for which sound sources might play an important role for receivers located at the adjoint function source location. At moderately high frequencies (Strouhal numbers around one) higher amplitudes for the adjoint Green's function appear with the M3 microphone location (40 degrees from the jet axis) mostly in the downstream region of the jet plume. Whereas at M5 (90 degrees from the jet axis) they are distributed all along the jet's shear layer. This is consistent with the idea that jet noise radiated to downstream observer locations comes primarily from a region near the end of the jet's potential core, while that at ninety degrees comes from a wider distribution of locations throughout the shear region.

The phase of adjoint Green's function also plays a decisive role, as can be seen from equation (14), spatially broad sound sources may not radiate efficiently as different parts of the sound source might cancel out. In Figure 6, as the adjoint source frequency increases, a directivity pattern close to the point source appears. Such an evolution of the source directivity with the frequency is not visible in Figure 5, for the observer location M3. This modification of the directivity might be caused by the point source being set too close to the absorbing boundary condtition, however this does not seem to affect the final solution as, apart for 3000 Hz, the adjoint method retrieves correctly the reference direct solution. Thus further efforts are required to verify the correctness of the computed adjoint fields as well as to properly interpret these results.

VIII.Conclusion

In this paper we have presented a formulation of the adjoint Green's function problem for the non-conservative form of the linearized Euler equations (LEE) and shown how it can be used within an acoustic analogy approach based on these equations to predict turbulent mixing noise from a turbulent jet. The most computationally intensive part of this process is numerically computing the adjoint Green's function.

Results computed for the adjoint Green's function for a demonstration test case of a round, near-sonic, unheated jet are presented using an adaptive high-order Discontinuous Galerkin finite element solver within Actran DGM [13]. A separate numerical solution is obtained for the direct Green's function of the LEE using an exsiting solver in Actran DGM. A vortical diffusive limiter is used to reduce the influence of spatially growing Kelvin – Helmholz waves on the desired bounded solution relevant for jet noise.

Results for the acoustic pressure computed by the two different methods are compared at five microphones whose locations are positioned where experimental data is available. Solutions from the two different methods agree well, except at around 2 -3 kHz where the exponential growing KH instability waves may still contaminate the results. Maps of the adjoint Green's function in the source region at two of these microphone locations are presented. These results can be used to distinguish regions in the flow where the unsteady source terms in the formulation can be expected to make significant contributions to the noise radiated to these observers.

Future work will compare the Green's functions computed using Actran DGM with those of reduced forms of the LEE, for example from approximating the mean flow as locally parallel. In addition, models for the statistics of the source terms in the LEE will be implemented to provide a full jet noise prediction capability in Actran DGM using the adjoint Green's function approach whose results can be compared with experimentally measured noise data. Future work will also include consideration of cases where solid surfaces exist near the jet to model installation effects.

Acknowledgments

The work of SJL was supported by the NASA Advanced Air Vehicles Program /High-Speed Flight Project. Dr. James Bridges is thanked for his technical support. Dr. Nick Georgiadis of NASA Glenn provided the RANS solution used in this work. The authors would like to thank Nvidia and SuperMicro for providing GraceHopper GH200 nodes used in the present simulations.

References

[1] M. Lighthill, "On sound generated aerodynamically. I General theory," *Proc. Roy. Soc., A221,* pp. 564-587, 1952.

[2] C. Bogey, C. Bailly and D. Juvé, "Computation of flow noise using source terms in linearized Euler's equations," *AIAA Journal, 40, No. 2,* pp. 235-243, 2002.

[3] C. Tam and L. Auriault, "Mean flow refraction effects on sound raidated from localized source in a jet," *J. Fluid Mech.,* pp. 149-174, 1998.

[4] P. Morse and H. Feshbach, Methods of theoretical Physics, McGraw-Hill, 1953.

[5] C. Tam and L. Auriault, "Jet mixing noise from fine-scale turbulence," *AIAA Journal,* vol. 37(2), pp. 145-153, 1999.

[6] E. Spieser and C. Bailly, "Sound propagation using and adjoint-based method," *Journal of Fluid Mechanics,* vol. 900, no. A5, pp. 1-25, 2020.

[7] S. Le Bras, G. Gabard and H. Bériot, "Direct and adjoint problems for sound propagation in non-uniform flows with lined and vibrating surfaces," *Journal of Fluid Mechanics,* vol. 953:A16, 2011.

[8] E. Spieser, C. Legendre and C. Bailly, "Acoustic modelling of the installation effects of a subsonic jet beneath a flat plate," in *28th AIAA/CEAS Aeroacoustics 2022 Conference*, Southampton, 2022-2858.

[9] E. Spieser, C. Bogey and C. Bailly, "Noise predictions of a Mach 0.9 round jet using tailored adjoint Green's functions," *Journal of Sound and Vibration,* vol. 548:117532.

[10] M. Goldstein and S. Leib, "The aeroacosutics of slowly diverging supersonic jets," *Journal of Fluid Mechanics,* vol. 600, pp. 291-337, 2008.

[11] S. Leib and M. Goldstein, "Hybrid source model for predicting high-speed jet noise," *AIAA Journal,* vol. 49(7), pp. 1324-1335, 2011.

[12] M. Goldstein, "A generalized acoustic analogy," *Journal of Fluid Mechanics,* vol. 488, pp. 315-333, 2003.

[13] Free Field Technologies division, Design & Engineering, Hexagon AB, Actran DGM 2025.2, 2025.

[14] C. Legendre, B. de Brye, S. Subramaniyam, B. Ganty, Y. Detandt and C. Bailly, "Towards large aeroacoustic applications thourgh a hybrid approach based on the Linearized Euler Equations," in *23rd Internatioanl Congress on Sound & Vibration*, Athens, Greece, 2016.

[15] J. Bridges and M. Wernet, "Establishing Consensus Turbulence Statistics for Hot Subsonic JEts," *AIAA 2010-3751,* 2010.

[16] C. Brown and J. Bridges, "Small Hot Jet Acoustic Rig Validation," NASA/TM 2006-214234, 2006.

[17] C. Nelson and G. Power, "CHSSI Project CFD-7: The NPARC Allicance Flow Simulation System," *AIAA 2001-0594,* 2001.

[18] R. Bush, G. Power and C. Towne, "WIND: The Production Flow Solver of the NPARC Alliance," *AIAA 98-0935,* 1998.

[19] C.-W. Shu and S. Osher, "Efficient implementation of essentially non-oscillatory shock-capturing schemes," *Journal of Computational Physics,* no. 77, pp. 469-471, 1988.